IOP Publishing Journal of Physics D: Applied Physics
J. Phys. D: Appl. Phys. **50** (2017) 375105 (7pp) https://doi.org/10.1088/1361-6463/aa8197

Spoof surface plasmons tunneling through an epsilon-near-zero material channel

Zhuo Li[1,3], Yunhe Sun[1], Hengyi Sun[1], Kuan Wang[1], Jiajia Song[1], Liangliang Liu[1,2], Xinlei Chen[1] and Changqing Gu[1]

[1] Key Laboratory of Radar Imaging and Microwave Photonics, Minister of Education, College of Electronic and Information Engineering, Nanjing University of Aeronautics and Astronautics, Nanjing, 211106, People's Republic of China
[2] The Research Center of Applied Electromagnetics, School of Electronic and Information Engineering, Nanjing University of Information Science and Technology, Nanjing, 210044, People's Republic of China
[3] State Key Laboratory of Millimeter Waves, Southeast University, Nanjing, 210096, People's Republic of China

E-mail: lizhuo@nuaa.edu.cn

Received 25 May 2017, revised 12 July 2017
Accepted for publication 24 July 2017
Published 24 August 2017

Abstract

In this paper, squeezing and tunneling of spoof surface plasmon polaritons (SSPPs) are realized by introducing an effective epsilon-near-zero (ENZ) material channel between two plasmonic waveguides constructed from dielectric filled rectangular waveguide etched with deep sub-wavelength periodical transverse slots on the upper wall. The tunneling frequency can be flexibly tuned by changing the relative permittivity of the effective ENZ material and the SSPPs can tunnel efficiently through a straight or an arbitrarily bent effective ENZ channel with ultra-low loss. This simple design holds great promise in significantly increasing the propagation length or arbitrarily tuning the propagation direction of the SSPPs in the microwave and terahertz frequencies.

Keywords: surface plasmon polaritons, tunneling, spoof surface plasmons, epsilon-near-zero material

(Some figures may appear in colour only in the online journal)

1. Introduction

Surface plasmon polaritons (SPPs) are surface waves tightly confined at the interface between metal and dielectric at optical frequencies [1–3]. SPPs have been widely used in sensors, plasmonic waveguide and miniaturization of photonic circuits due to great field enhancement and deep sub-wavelength field confinement [4–7]. However, at microwave and terahertz frequencies, SPPs cannot be supported at this interface since metal behaves like a perfect electric conductor (PEC). In 2004, Pendry and co-workers proposed a new concept of spoof surface plasmon polaritons (SSPPs) to mimic the SPPs characteristics at lower frequencies by etching the metal surface with sub-wavelength periodical grooves or holes [8, 9]. Experimental verifications have also been conducted later on [10]. The SSPPs have inherited most of the exotic features of real SPPs and a large number of plasmonic transmission structures based on SSPPs have been presented for the routing of microwave and terahertz waves with high field confinement and enhancement [11–15]. At optical frequencies, tunneling of the SPPs has already been realized [16]. However, to the best of our knowledge, squeezing and tunneling of spoof surface plasmon polaritons at microwave or terahertz frequencies have not been reported yet because ENZ or effective ENZ materials cannot be easily incorporated in conventional SSPPs waveguides.

In recent years, Engheta *et al* have proposed the concept of tunneling of electromagnetic energy through ultra-narrow channels and bends filled with ENZ or effective ENZ materials [17–21]. Later on, squeezing and tunneling energy in an ultra-narrow waveguide were verified experimentally [22]. In 2016, Engheta numerically demonstrated that waves in a rectangular waveguide can tunnel through an effective ENZ material realized with only positive dielectric based on the effective medium theory in a bounded waveguide [23].

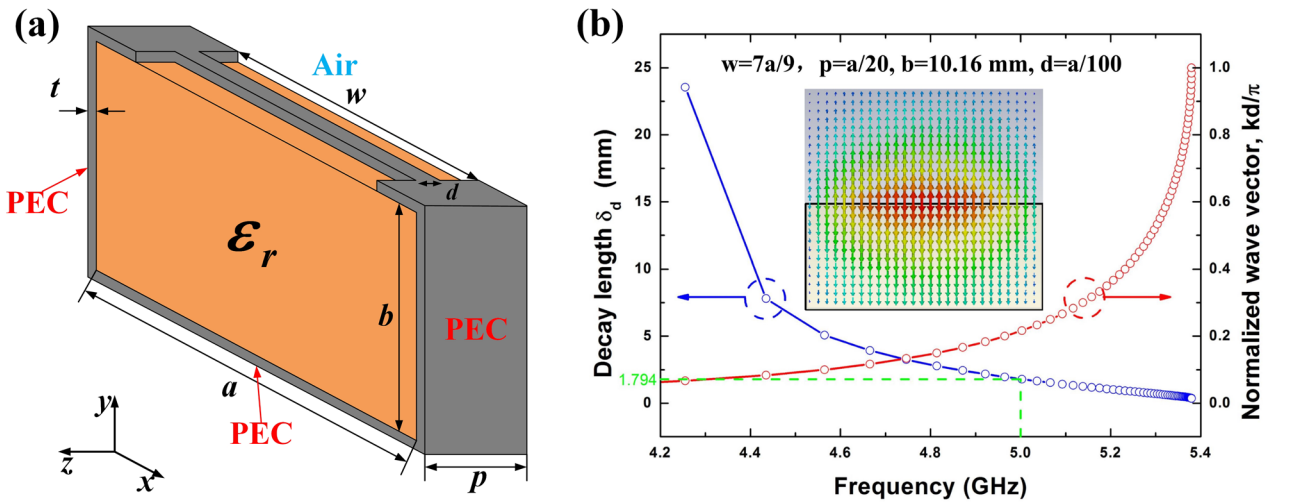

Figure 1. (a) Sketch of the unit cell of the plasmonic waveguide. (b) The dispersion curve of the SSPPs (the red line) and the corresponding decay length (the blue line) in the -*y* direction, and the electric lines of force of the eigenmode in the cross section (*xy* plane) are shown in the inset.

In this work, borrowing nearly the same idea from Engheta, we realize the squeezing and tunneling of SSPPs through a straight or an arbitrarily bent effective ENZ channel bridged between two plasmonic waveguides. The trick is that the judiciously designed plasmonic waveguide not only support high efficiency and broadband transmission of the SSPPs, but can be seamlessly connected with an effective ENZ channel to realize energy squeezing and tunneling as well. In this way, the propagation length of the SSPPs can be significantly increased and the power flow can be directed towards any direction.

2. Design of the plasmonic waveguide

To begin with, the dispersion characteristics of the SSPPs supported on the proposed plasmonic waveguide are investigated. As shown in figure 1(a), the unit cell with the period p of the plasmonic waveguide is assumed to be filled with an isotropic and homogeneous dielectric of relative permittivity $\varepsilon_r = 4$, and relative permeability $\mu_r = 1$. The dimensions in the cross section are $a = 22.86$ mm and $b = 10.16$ mm respectively, and the thickness of the metal wall is set as $t = 0.05$ mm. The upper metal wall of the unit cell is partially subtracted and replaced with a symmetrically positioned metallic strip with lateral length w and width d. The dispersion curves and field distributions of the SSPPs supported on the unit cell are calculated by the eigenmode solver of the commercial software CST microwave studio. The dispersion curve and the corresponding decay length δ_d are both shown in figure 1(b), in which the decay length is defined as the penetration depth of the SSPPs into the plasmonic waveguide vertically in the -y direction when the magnitude of the electric field $|\mathbf{E}|$ right at the interface decays to $|\mathbf{E}|\,e^{-1}$ that $|\mathbf{E}|\,e^{-k_y\delta_d} = |\mathbf{E}|\,e^{-1}$, in which $k_y = \sqrt{k_z^2 - \varepsilon_r k_0^2}$ and ε_r is the relative permittivity of the medium filled in the rectangular waveguide. It is obvious from figure 1(b) that the higher the operating frequency is, the tighter field confinement can be obtained. The decay length δ_d is far less than the height of the waveguide b when frequency approaches the asymptotic frequency of the SSPPs. The decay length $\delta_{d,5\ \mathrm{GHz}} = 1.794$ mm at 5 GHz is less than $b = 10$ mm and shown as the green dotted line in figure 1(b). From the eigenmode electric field distributions in the *xy* plane of the unit cell in figure 1(b), we can clearly observe that the fields are tightly confined at the interface between the dielectric in the waveguide and the air above. And with the help of the metallic strip, the electric lines of force point towards opposite directions in the dielectric and air, perfectly mimicking the behavior of the real SPPs at optical frequencies.

Then, we analyze the dispersion relations of the SSPPs with the variations of four parameters (w, p, b, d/p) in figure 2. From figures 2(a) and (b), we can clearly observe that the asymptotic frequency of the SSPPs can be tuned by the lateral length w of the strip and the period p of the unit cell. With the decrease of w from a to 0, the asymptotic frequency of the SSPPs increases and approaches infinity considering that the unit cell itself becomes a segment of a conventional rectangular waveguide which has no asymptote above its cutoff frequency. Thus, we can fully utilize this characteristic to smoothly convert the TE_{10} mode to the SSPPs with gradient increase of w. In addition, the dispersion relations are not sensitive to the variations of the height b of the waveguide and the width ratio d/p of the metallic strip according to figures 2(c) and (d). Thus, analogous SSPPs can be expected to be supported on the substrate integrated waveguide with periodical transverse slots on the surface. And, we can choose proper value of the ratio d/p not to complicate the structure fabrication.

Thus, we can use the unit cell in figure 1(a) to construct a plasmonic waveguide shown in figure 3(a). Although nearly the same structure has been investigated in [24], the SSPPs supported on this structure have not been clarified and analyzed in detail. The whole waveguide is filled with an isotropic and homogeneous dielectric with relative permittivity $\varepsilon_r = 4$, and composed of three regions with the length $l_1 = l_5 = a$, $l_2 = l_4 = 2a$ and $l_3 = 3a$ respectively. Region I is a conventional rectangular waveguide. Region II is the mode

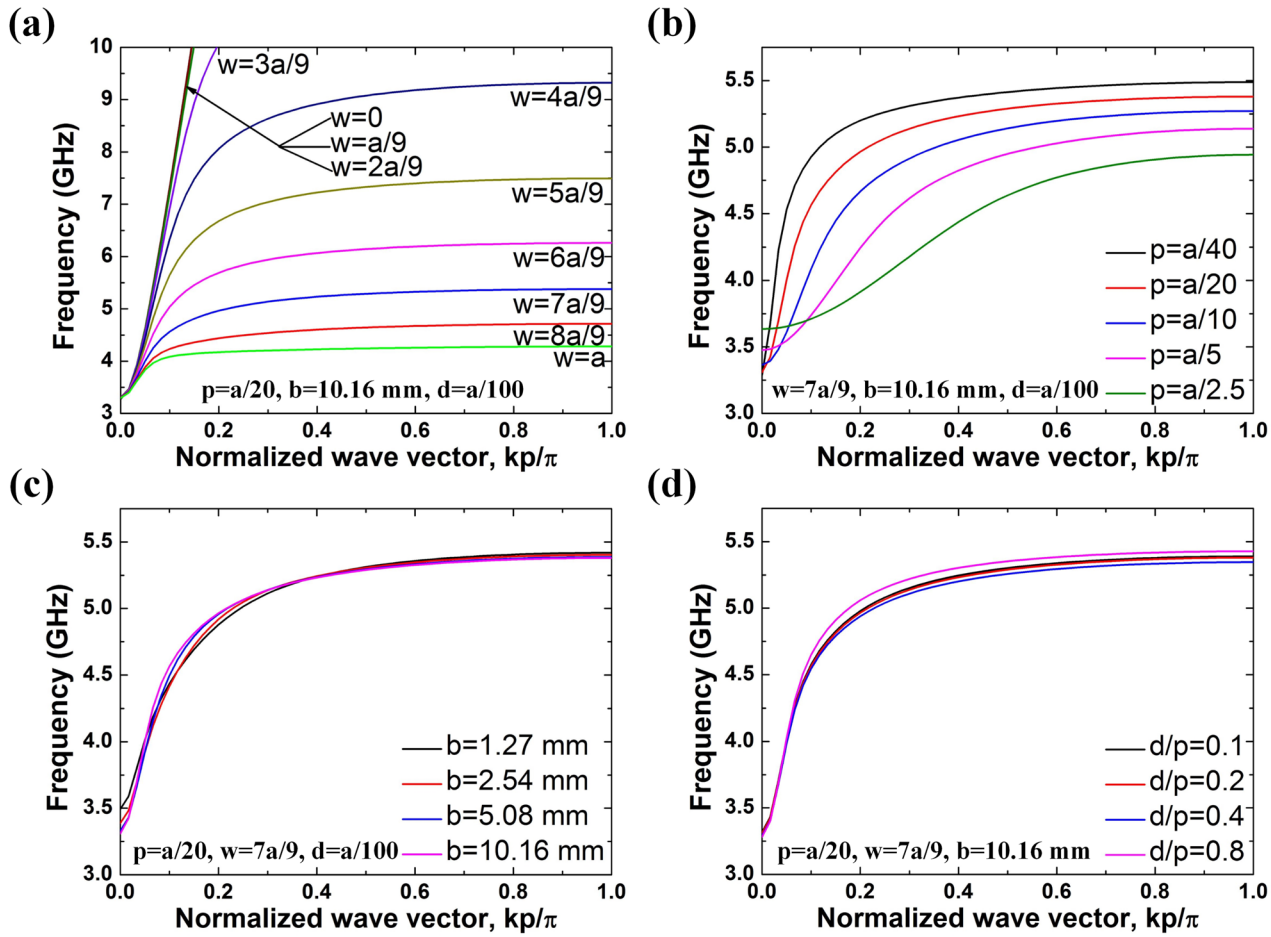

Figure 2. (a)–(d) The evolution of dispersion curves for the SSPPs supported on the unit cell with the variation of w, p, b and d/p, in which other parameters are fixed.

conversion section with gradient increasing width strips from $w = 0$ to $w = 7a/9$, which can realize smooth mode conversion from the TE_{10} mode in the rectangular waveguide to the SSPPs. Region III is the plasmonic waveguide. Here, the period of the strip is set as $p = a/20$ and the width of each strip is set as $d = a/100$. In order to obtain superior transmission performance and appropriate bandwidth, the lateral length of the strips in Region III is set as $w = 7a/9$. The simulated transmission coefficient S_{21} (red curve) and reflection coefficient S_{11} (black curve) are shown in figure 3(b), from which we can observe that the SSPPs spectrum lies between 3.28 GHz and 5.33 GHz. The asymptotic frequency of the plasmonic waveguide 5.33 GHz agrees quite well with that in the dispersion curve. In the passband, S_{11} is lower than -15 dB from 3.32 GHz to 5.24 GHz indicating that no more than 6% power is reflected. Figures 3(c)–(e) show the distributions of the y-component of electric fields in the yz ($x = 0$ mm) and xz ($y = 8$ mm, 12 mm) planes at 5 GHz respectively. It is evident from figure 3(c)that the TE_{10} wave is smoothly converted into the SSPPs and tightly confined at the interface between the plasmonic waveguide and the air above. Figures 3(d) and (e) show the E_y distributions inside and outside of the plasmonic waveguide in two xz planes, in which the SSPPs exhibit great field enhancement compared with the TE_{10} waves in the rectangular waveguide on both sides. The simulated wavelength of the SSPPs 10.51 mm ($0.175\lambda_0$) obtained from the field distributions on the plasmonic waveguide agrees quite well with the theoretically predicted wavelength $\lambda_{spp,\ 5\ GHz} = 2\pi/k_{spp} = 10.55$ mm ($0.176\lambda_0$) obtained from the simulated dispersion curve, in which λ_0 is the free space wavelength at the operating frequency $f_0 = 5$ GHz.

3. Tunneling of SSPPs in a straight effective ENZ channel

According to the former work [23], the tunneling of TE_{10} mode in a conventional rectangular waveguide can be realized by incorporating an effective ENZ material channel. Here, borrowing nearly the same idea, we would test if the proposed SSPPs could also tunnel through an effective ENZ channel. The plasmonic waveguide shown in figure 3(a) is cut in the middle with one half connected with the input port and the other half connected with the output port. Then we connect these two halves with a narrow channel filled with a positive dielectric of relative permittivity ε_{r2}, which acts as an effective ENZ material. First we consider three straight narrow channels, including an inverted U-shaped channel (Model 1), an H-shaped channel (Model 2) and a U-shaped channel (Model 3) shown as the purple regions in figures 4(a)–(c).

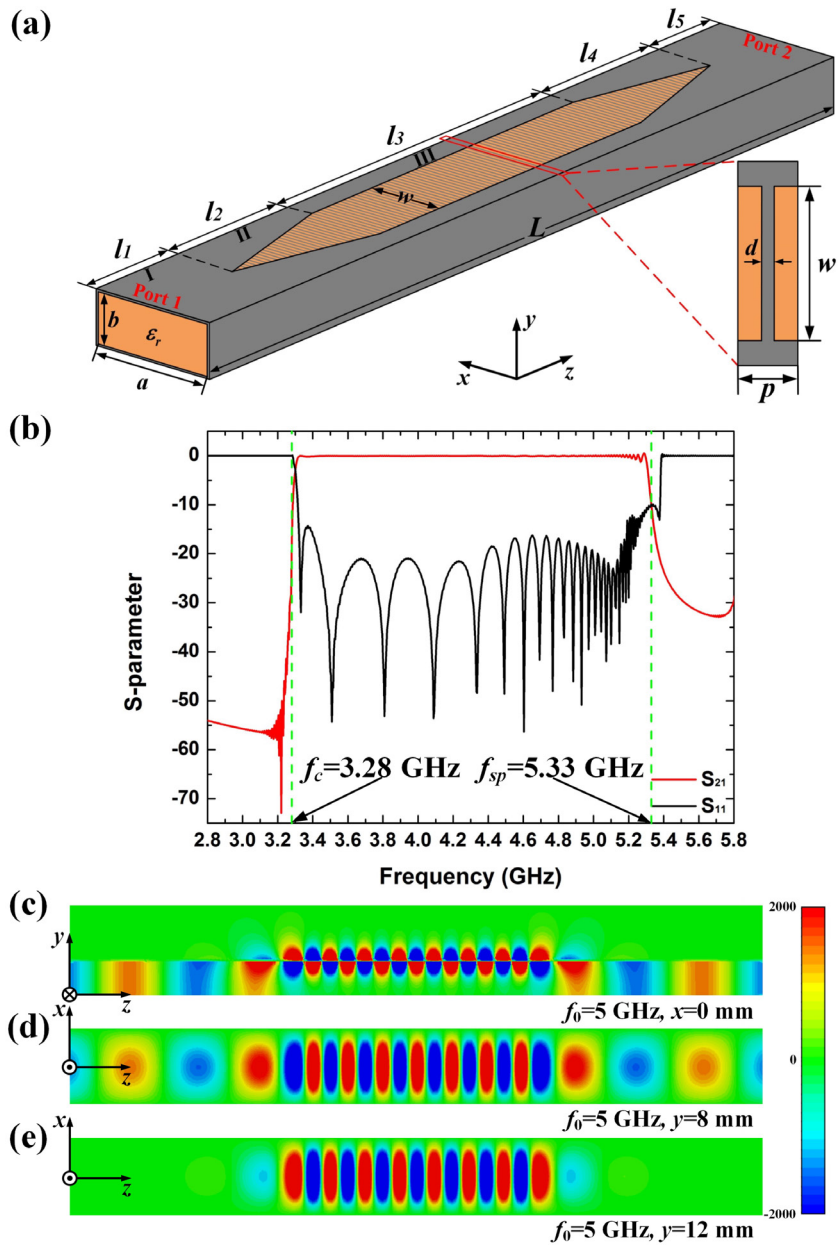

Figure 3. (a) The schematic illustration of the plasmonic waveguide and the front view of the unit cell. (b) The S-parameters of the plasmonic waveguide. (c)–(e) The simulated E_y (V m^{-1}) distributions in the yz plane ($x = 0$ mm) and two xz planes ($y = 8$ mm, 12 mm) at 5 GHz, respectively.

The lengths of Regions I, II, and III are the same with those set in figure 3(a) and the total length L of Model 1, 2, and 3 is $16a$. The plasmonic waveguides on both sides are filled with a dielectric with relative permittivity $\varepsilon_{r1} = 4$ (orange region), and the narrow channel is filled with a dielectric with relative permittivity $\varepsilon_{r2} = 2.4$ (purple region). The height of the channel in the y direction is set as $w_c = b/4$. A series of thin metallic strips with width $a/100$ are placed uniformly along the interface between these two dielectrics. As stated in [25], the effective relative permittivity of a dielectric with regard to mode TE_{10} can be calculated by $\varepsilon_e = \varepsilon_r - \lambda_0^2/4a^2$, in which ε_r is the relative permittivity of the dielectric filled in the waveguide, a is the lateral length of the waveguide, and λ_0 is the free-space wavelength. Thus, at 4.24 GHz, the effective relative permittivity of these two dielectrics are $\varepsilon_{\text{eff } r1} = 1.6$ and $\varepsilon_{\text{eff } r2} = 0$ respectively. As expected in figure 4(e), two transmission peaks occur in the simulated S-parameter curves of all three models, in which the first peak at 4.24 GHz is associated with the tunneling effect of the SSPPs through the effective ENZ channel and the second transmission peak is due to the Fabry–Perot effect. Although the three channels are positioned quite differently along the y direction, they exhibit nearly the same tunneling effect at 4.24 GHz and slightly different Fabry–Perot effect at 4.38 GHz from the agreement degrees of the S-parameter curves. To confirm that the second peak is due to the Fabry–Perot effect, we consider the same waveguide with a longer channel ($l_4 = 5a$) shown in figure 4(d). As expected, the second transmission peak redshifts due to lower resonant frequency of the Fabry–Perot effect with the first transmission peak unchanged, which is the

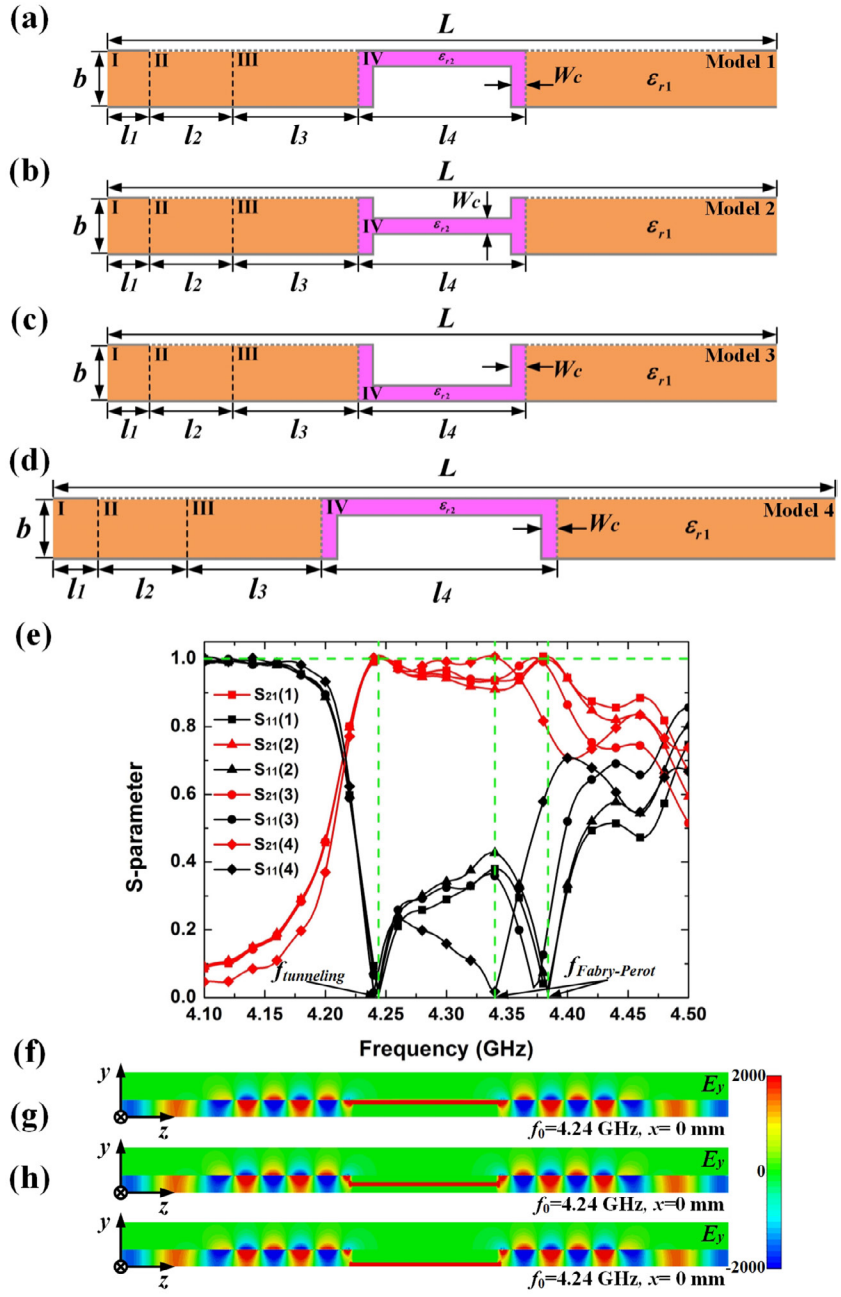

Figure 4. Tunneling of SSPPs in a straight effective ENZ channel: (a)–(c) the cut planes ($x = 0$ mm) of two plasmonic waveguides connected by an inverted U-shaped channel, an H-shaped channel and a U-shaped channel respectively, in which $l_1 = a$, $l_2 = 2a$, $l_3 = 3a$ and $l_4 = 4a$. (d) The cut plane ($x = 0$ mm) of two plasmonic waveguides connected by a longer inverted U-shaped channel. (e) S-parameters of the four models in (a)–(d). (f)–(h) The simulated E_y (V m^{-1}) distributions in the plane ($x = 0$ mm) of the three models in (a)–(c).

tunneling frequency. The simulated near-field distributions of E_y at 4.24 GHz on the yz plane ($x = 0$ mm) of Models 1–3 are shown in figures 4(f)–(h). It can be observed that the TE_{10} mode is smoothly converted to the SSPPs and tightly confined at the interface between the dielectric in the rectangular waveguide and the air above. When the SSPPs approach the interface between the plasmonic waveguide and the effective ENZ channel, the energy of the SSPPs is squeezed and tunnel through the channel and replicate themselves at the other side of the channel. The SSPPs are directly squeezed and tunnel through the effective ENZ material channel due to the high confinement and localization characteristics of the SSPPs. It seems that there are some fields outside the waveguide, however, most energy tunnel through the effective ENZ channel efficiently.

To test the flexibility of the tunneling frequency tuning of SSPPs, we consider another case when the effective ENZ channel is filled with a dielectric with relative permittivity $\varepsilon_r = 1.72$ (tunneling frequency at 5 GHz) and all other parameters keep unchanged. The simulated E_y distributions in the yz plane ($x = 0$ mm) of all three models are shown in figures 5(a)–(c). It can be observed that although at 5 GHz the SSPPs waves exhibit much shorter decay length and tighter confinement they can still tunnel through the three channels

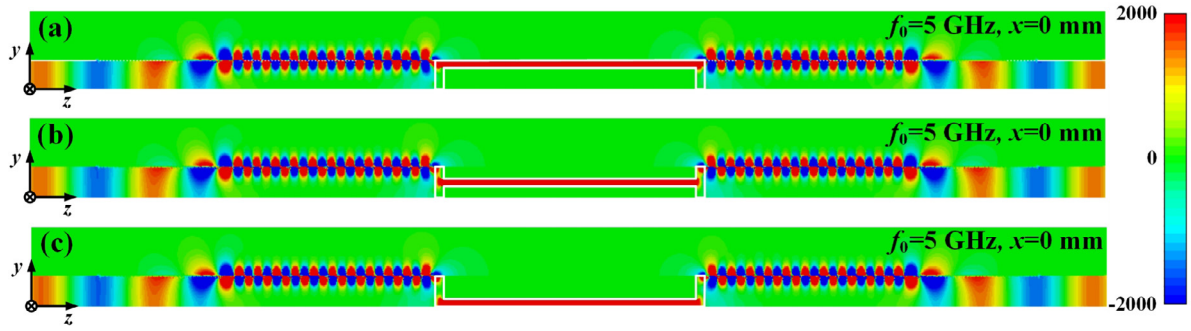

Figure 5. Tunneling of SSPPs in a straight effective ENZ channel filled with a dielectric with relative permittivity $\varepsilon_r = 1.72$. (a)–(c) The simulated E_y (V m^{-1}) distributions in the yz plane ($x = 0$ mm) of Models 1–3 in figures 4(a)–(c) at 5 GHz.

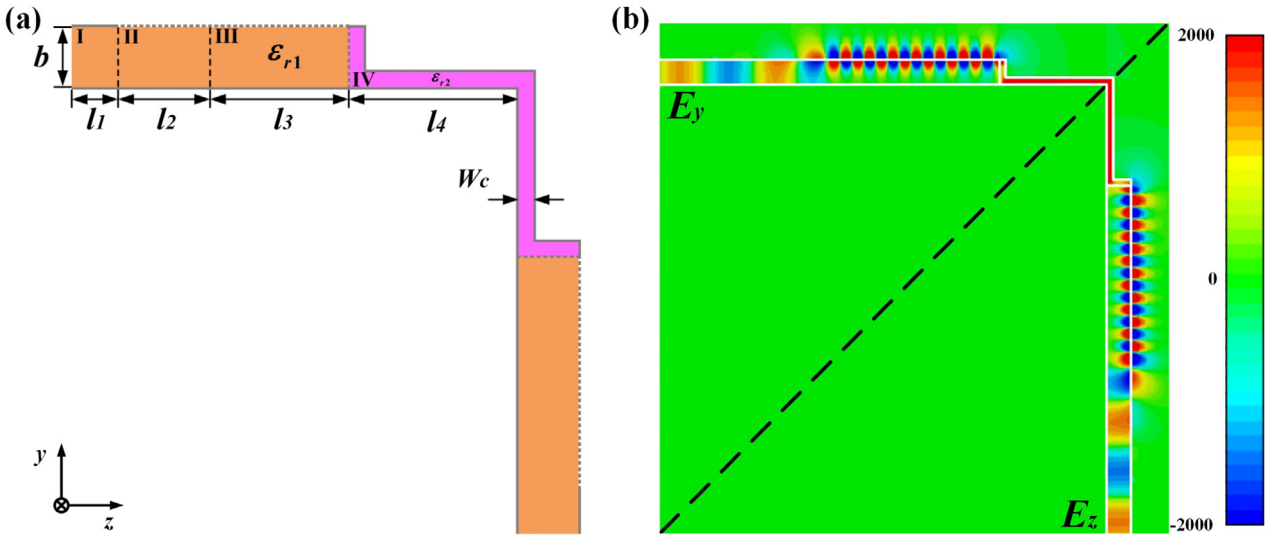

Figure 6. Tunneling of SSPPs in a 90-degree-bent effective ENZ channel. (a) Two plasmonic waveguides are connected by a 90-degree-bent channel. (b) The simulated near electric-field distributions in the yz plane at $x = 0$ mm.

efficiently. According to the analysis of the unit cell, tight confinement and localization of the SSPPs can be still obtained at high operating frequency. Thus, at 5 GHz, the SSPPs can still squeeze into the effective ENZ channel and then tunnel through it.

4. Tunneling of SSPPs in a bent effective ENZ channel

To further validate the performance of the tunneling of SSPPs through arbitrarily bent channel, a 90-degree-bent effective ENZ channel is designed as shown in figure 6(a). The dielectrics in the plasmonic waveguide and the dimensions of the channel keep all the same as those in the third case in figure 5. The whole structure is symmetrical about the black dashed line in figure 6(b) and the half length of the ENZ channel is $l_4 = 2a$. The simulated E_y distributions on the left-hand side of the dashed line and E_z distributions on the right-hand side of the dashed line at 5 GHz are shown in figure 6(b), it is obvious that the SSPPs efficiently squeeze into and tunnel through the bent effective ENZ channel with ultra-low loss. Thus, we believe this judiciously designed plasmonic waveguide can realize the tunneling of SSPPs in arbitrarily bent effective ENZ channel.

5. Conclusions

In summary, with the same tunneling idea of TE_{10} mode in conventional rectangular waveguide, squeezing and tunneling of SSPPs are realized by bridging two judiciously designed plasmonic waveguides with an effective ENZ channel. The tunneling frequency can be flexibly and easily tuned by changing the relative permittivity of the effective ENZ material and the SSPPs can tunnel efficiently through a straight or an arbitrarily bent effective ENZ channel with ultra-low loss. Although the feasibility of using the structure is only exhibited in the GHz region, we believe that the structure can be scaled down and extended to higher frequencies regime, such as millimeter-wave and terahertz regime. Thus, this simple design may have potential applications in increasing the propagation length and tuning the propagation direction of the SSPPs at microwave and terahertz frequencies.

Acknowledgments

This work has been partially supported by Foundation of the Fundamental Research Funds for the Central Universities (NS2016039); State Key Laboratory of Millimeter Waves,

Southeast University, China (K201603); Natural Science Foundation of Jiangsu Province (BK20151480); Jiangsu Innovation Program for Graduate Education (KYLX16_0370); The Priority Academic Program Development of Jiangsu Higher Education Institutions and the talent start-up fund of Nanjing University of Information Science & Technology; Fundation of Graduate Innovation Center in NUAA (kfjj20170411); Fundation of Graduate Innovation Center in NUAA (kfjj20170414).

References

[1] Barnes W L, Dereux A and Ebbesen T W 2003 Surface plasmon subwavelength optics *Nature* **420** 824–30
[2] Maier S A 2007 *Plasmonics: Fundamentals and Applications* (Berlin: Springer) (https://doi.org/10.1007/0-387-37825-1)
[3] Pitarke J M, Silkin V M, Chulkov E V and Echenique P M 2007 Theory of surface plasmons and surface plasmon polaritons *Rep. Prog. Phys.* **70** 1
[4] Brolo A G *et al* 2004 Surface plasmon sensor based on the enhanced light transmission through arrays of nanoholes in gold films *Langmuir* **20** 4813–5
[5] Fang N, Lee H, Sun C and Zhang X 2005 Subdiffraction-limited optical imaging with a silver superlens *Science* **308** 534–7
[6] Ozaki M, Kato J and Kawata S 2011 Surface-plasmon holography with whitelight illumination *Science* **332** 218–20
[7] Oulton R F *et al* 2008 A hybrid plasmonic waveguide for subwavelength confinement and long-range propagation *Nat. Photon.* **2** 496–500
[8] Pendry J B, Martin-Moreno L and Garcia-Vidal F J 2004 Mimicking surface plasmons with structured surfaces *Science* **305** 847–8
[9] Garcia-Vidal F J, Martin-Moreno L and Pendry J B 2005 Surfaces with holes in them: new plasmonic metamaterials *J. Opt. A: Pure Appl. Opt.* **7** S97
[10] Hibbins A P, Evans B R and Sambles J R 2005 Experimental verification of designer surface plasmons *Science* **308** 670–2
[11] Ma H F *et al* 2014 Broadband and high-efficiency conversion from guided waves to spoof surface plasmon polaritons *Laser Photon. Rev.* **8** 146–51
[12] Gao X *et al* 2014 An ultra-wideband surface plasmonic filter in microwave frequency *Appl. Phys. Lett.* **104** 191603
[13] Liu L L *et al* 2014 Multichannel composite spoof surface plasmon polaritons propagating along periodically corrugated metallic thin films *J. Appl. Phys.* **116** 013501
[14] Liu L L *et al* 2015 Smooth bridge between guided waves and spoof surface plasmon polaritons *Opt. Lett.* **40** 1810–3
[15] Liu L L *et al* 2015 High-efficiency transition between rectangular waveguide and domino plasmonic waveguide *AIP Adv.* **5** 027105
[16] Darmanyan S A and Zayats A V 2003 Light tunneling via resonant surface plasmon polariton states and the enhanced transmission of periodically nanostructured metal films *Phys. Rev.* B **67** 035424
[17] Silveirinha M and Engheta N 2006 Tunneling of electromagnetic energy through subwavelength channels and bends using ε-near-zero materials *Phys. Rev. Lett.* **97** 157403
[18] Silveirinha M G and Engheta N 2007 Theory of supercoupling, squeezing wave energy, and field confinement in narrow channels and tight bends using ε near-zero metamaterials *Phys. Rev.* B **76** 245109
[19] Alu A, Silveirinha M G and Engheta N 2008 Transmission-line analysis of ε-near-zerofilled narrow channels *Phys. Rev.* E **78** 016604
[20] Alu A and Engheta N 2008 Dielectric sensing in ϵ-near-zero narrow waveguide channels *Phys. Rev.* B **78** 045102
[21] Engheta N 2013 Pursuing near-zero response *Science* **340** 286–7
[22] Edwards B *et al* 2008 Experimental verification of epsilon-near-zero metamaterial coupling and energy squeezing using a microwave waveguide *Phys. Rev. Lett.* **100** 033903
[23] Della Giovampaola C and Engheta N 2016 Plasmonics without negative dielectrics *Phys. Rev.* B **93** 195152
[24] Liu J, Jackson D R and Long Y 2011 Modal analysis of dielectric-filled rectangular waveguide with transverse slots *IEEE Trans. Antennas Propag.* **59** 3194–203
[25] Li Z *et al* 2017 Effective surface plasmon polaritons induced by modal dispersion in a waveguide *Phys. Rev. Appl.* **7** 044028